PHYSICAL REVIEW B VOLUME 24, NUMBER 4 15 AUGUST 1981

Augmented-plane-wave to Gaussian-orbital conversion procedure: One-electron states and Compton profiles of fcc neon

A. K. Ray and S. B. Trickey
Quantum Theory Project, Department of Physics, University of Florida, Gainesville, Florida 32611

(Received 17 February 1981)

The methodology of using symmetrized augmented-plane-wave results as input for the Wang-Callaway linear combination of Gaussian-type orbitals (LCGTO) band-structure codes is developed and applied to fcc Ne as an example. At a cost of less than a 20% increase in computing time (compared with a regular LCGTO run), one obtains both muffin-tin and non-muffin-tin results. Certain technical advantages regarding basis-set inadequacies and avoidance of spurious self-consistencies also accrue with this hybrid method.

I. INTRODUCTION

In its canonical form, the augmented-plane-wave (APW) method[1] for determining crystalline band energies ϵ_{jk} and orbitals ϕ_{jk} is restricted to periodic potentials of muffin-tin (MT) form. With local spherical symmetry inside spheres centered at the nuclear sites and a constant value elsewhere, such a potential admits of a solution corresponding to plane waves in the external or flat region and to a simple angular momentum (partial-wave) decomposition inside each APW sphere. As is well known, the result is a technique which is very efficient, reliable, and much used in computation of crystalline energy bands, cohesive energies, etc. Another often-used scheme, the Korringer-Kohn-Rostoker (KKR) method,[2] is also employed almost exclusively with the MT approximation.

The removal of MT effects has long been a concern. The "nonflat" contributions (i.e., those non-MT contributions occurring exterior to the APW spheres) apparently were first considered by Schlosser and Marcus.[3] Subsequently, a number of other authors[4–12] have treated the problem in diverse ways, generally involving Fourier expansions, partial-wave expansions coupling nonzero m's ($|m| \leq l$), perturbation theory to low order, etc. The issue has also been confronted in the KKR context.[13] Nevertheless, the bulk of work to date which has used APW or KKR techniques has been in MT form.

Concurrently, entirely distinct electronic-structure methodologies have been developed[14–16] which do not involve the MT assumption. Methods involving Gaussian-type orbitals (GTO's) have been of particular interest to us, since a variety of molecular[17,18] and film[19] codes using GTO's are in active development and use in this project. A particularly appealing package of crystalline codes is the Wang-Callaway[20] or LSU (hereafter) linear combination of GTO's (LCGTO) package because of its availability and extensive utilization by its originators.

We report here the formulas necessary to utilize symmetrized-APW (SAPW) results as input to the LSU package and comment on certain technical aspects of the computational procedure. As an example, we report non-MT energy bands and Compton profiles for fcc Ne and compare them with our earlier MT results.[21,22] We find the SAPW followed by LCGTO strategy to give both converged MT and non-MT results of comparable quality in less than 20% more computational time than the calculation from scratch of the non-MT results alone. Among the benefits of this modest increment of cost are the following: (a) generation of MT results for comparison with other MT calculations; (b) direct assessment of non-MT effects; (c) provision of a realistic starting potential for the LSU code and, therefore, a reduction in the possibility that the latter will be "hung" in a false minimum during the self-consistent iteration process; (d) establishment of an independent test for basis-set inadequacies early in the LGCTO portion of the process. We elaborate on these benefits in later portions of the paper.

II. METHODOLOGY

The effective Schrödinger equation which determines the one-electron orbitals $\psi_n(\vec{k}, \vec{r})$ and band

©1981 The American Physical Society

energies $E_n(\vec{k})$ is

$$[-\nabla^2 + V(\vec{r})]\psi_n(\vec{k},\vec{r}) = E_n(\vec{k})\psi_n(\vec{k},\vec{r}) \,. \tag{2.1}$$

Here and throughout we employ rydberg atomic units. The potential $V(\vec{r})$ contains the Coulomb potentials for the electrons interacting with the fixed nuclei of the system and with one another, plus an exchange-correlation contribution represented in the $X\alpha$ local approximation[23]:

$$V(\vec{r}) = -\sum_{\mu} \frac{2Z}{|\vec{r}-\vec{R}_\mu|} + 2\int \frac{\rho(\vec{r}\,')}{|\vec{r}-\vec{r}\,'|} d\vec{r}\,' - 6\alpha \left[\frac{3}{8\pi}\rho(\vec{r})\right]^{1/3} \,. \tag{2.2}$$

In the muffin-tin approximation, the potential and charge density are approximated by their spherical averages inside each muffin-tin sphere and by constant values outside.

In the LCGTO approach,[20] the Bloch function is expanded in a set of tight-binding basis functions $\phi_i(\vec{k},\vec{r})$:

$$\psi_n(\vec{k},\vec{r}) = \sum_i c_{ni}(\vec{k})\phi_i(\vec{k},\vec{r}) \,. \tag{2.3}$$

The ϕ_i's are constructed in turn as properly phased linear combinations of Gaussian orbitals u_i placed on the lattice sites of the system:

$$\phi_i(\vec{k},\vec{r}) = N^{-1/2}\sum_{\mu} e^{i\vec{k}\cdot\vec{R}_\mu} u_i(\vec{r}-\vec{R}_\mu) \,. \tag{2.4}$$

Here N is the number of unit cells in the periodic volume and the u_i's are given by

$$u_i(\vec{r}) = N_i r^{l_i} e^{-\zeta_i r^2} \mathscr{K}_{l_i,j}(\hat{r}) \,, \tag{2.5}$$

where N_i is a normalization constant and $\mathscr{K}_{l_i,j}(\hat{r})$ is a Kubic harmonic of order l_i and type j, normalized to unity with respect to integration over solid angles.

The use of this basis ansatz yields a secular problem which contains integrals of $V(r)$ and $\rho(r)$ that are particularly amenable to treatment by lattice Fourier-transform techniques. The LSU code uses Fourier coefficients of the Coulomb potential $V_C(\vec{K}_s)$, the exchange-correlation potential $V_{\text{xc}}(\vec{K}_s)$, the density $\rho(\vec{K}_s)$, and the inverse square of the cube root of the density $\rho^{-2/3}(\vec{K}_s)$. The muffin-tin form of the augmented-plane-wave output makes it rather simple to generate these Fourier coefficients in a form appropriate for use as input to the rest of the LSU code.

We define the Fourier coefficients of a function $f(\vec{r})$ (in accordance with the Wang-Callaway normalization convention), as

$$f(\vec{K}) = \frac{1}{N\Omega}\int_{\text{PV}} f(\vec{r})\exp(-i\vec{K}\cdot\vec{r})d\vec{r} \,, \tag{2.6}$$

where PV denotes the periodic volume (comprised of N unit cells, each of volume Ω). Thus, if $f(\vec{r})$ has the periodicity of the lattice,

$$f(\vec{K}) = \frac{1}{\Omega}\int f(\vec{r})\exp(-i\vec{K}\cdot\vec{r})d\vec{r} \,.$$

For $f(\vec{r})$ of MT form and one atom per unit cell, we have

$$f_{\text{MT}}(\vec{r}) = \begin{cases} f(r), & 0 \le r \le R_s \\ f_0, & \text{a constant for } r \ge R_s \\ & \text{in the unit cell.} \end{cases}$$

Thus, for $K \neq 0$,

$$f_{\text{MT}}(K) = \frac{1}{\Omega}\left[\int_{\text{sph}} f(r)e^{-i\vec{K}\cdot\vec{r}}d\vec{r} + \int_{\text{ext}} f_0 e^{-i\vec{K}\cdot\vec{r}}d\vec{r}\right] = \frac{1}{\Omega}\left[\frac{4\pi}{K}\int_0^{R_s} f(r)r\sin Kr\,dr - 4\frac{\pi}{K}f_0 R_s^2 j_1(KR_s)\right] \tag{2.7}$$

In (2.7) $j_1(KR_s)$ is the spherical Bessel function of the first kind. For $\vec{K}=0$, we find

$$f(0) = \frac{1}{\Omega}\left[4\pi\int_0^{R_s} f(r)r^2dr + f_0(\Omega - \tfrac{4}{3}\pi R_s^3)\right] \,. \tag{2.8}$$

In an SAPW calculation, we generate the self-consistent muffin-tin potential, exchange potential, and charge density. Since the LSU code requires $V_C(K)$ separately from $V_{\text{xc}}(K)$, we construct the Coulomb contribution in Ω to $V_{\text{MT}}(r)$ by simple subtraction:

$$V_{C,\text{MT}}(\vec{r}) = V_{\text{MT}}(\vec{r}) - V_{\text{xc}}(\vec{r}) \,. \tag{2.9}$$

The quantity $\rho_{\text{MT}}^{-2/3}(r)$ is trivial to construct. Application of Eqs. (2.7) and (2.8) is then straightforward, and one generates the needed starting Fourier coefficients readily. A minor technical point (which, in fact, proved frustrating to us at first) is that the LSU code assumes that the Fourier coefficients stored for the exchange-correlation potential $V_{\mathrm{xc}}(K)$ are for $\alpha = 1.0$. Since most of our APW calculations are for other values of α, it is necessary to remember to scale the calculated $V_{\mathrm{xc,MT}}(K)$ by α^{-1} before storing them.

The integrals to R_s were done on the 441-point Herman-Skillman[24] mesh by five-point Newton-Cotes quadrature. Each integral was evaluated to upper limits that were from six Herman-Skillman points inside R_s through five points outside, followed by eleven-point interpolation of the value onto R_s itself.

To hasten the convergence of the reciprocal-lattice expansion of the Coulomb potential, the LSU code employs an Ewald procedure.[25] A superposition of atomic screening potentials $V_e(r) = \sum_\mu V_a(r - R_\mu)$, where

$$V_a(r) = -\frac{2Z}{r}\exp(-\beta_1 r^2) - \frac{\beta_2}{r}[\exp(-\beta_1 r^2) - \exp(-\beta_3 r^2)] , \tag{2.10}$$

is added to and subtracted from the Coulomb potential in each cell. As written, the LSU code fits the constants β_i (by an empirical procedure described by Wang and Callaway[25]) to the crystal potential which arises from a superposition of free-atom wave functions. For convenience, we elected to fit the β_i parameters to the intrasphere APW Coulomb potential. The results do not differ materially from those found by starting from the free-atom superpositions.

III. APPLICATION

APW calculations have been reported from this project[21,22] on the cohesive energy and Compton profile of fcc Ne in the $X\alpha$ model. Subsequently Khan and Callaway[26] (hereafter KC) reported LCGTO-$X\alpha$ calculations of the fcc Ne energy bands. They gave special emphasis to the need for large values of $\alpha(>1)$ to achieve decent agreement with the experimental value of the band gap. The opportunity therefore exists both to test the results of APW-to-LCGTO procedure (hereafter APW-GTO) against the KC results and to explore non-MT effects in the Ne crystalline Compton profile.

All the calculations reported here used the 12*s*, 8*p*,3*d* GTO basis employed by KC.[27] Because the orbital exponents could not be listed (due to space limitations) in Ref. 26, they are given in Table I. This basis yields Hamiltonian and overlap matrices of dimension 51 at a general point in the Brillouin zone (BZ). In the course of selecting a basis we tried first a 9*s*,6*p*,3*d* set—which turned out to have a peculiar feature: It obliterated the 3*s*-like state at Γ. As we had the SAPW result for the eigenvalue associated with that state, it was immediately clear that the smaller basis was deficient. Although the deficiency would be obvious in Ne even without having the SAPW bands, this experience points to an unanticipated advantage in the APW-GTO procedure. For a less familiar solid, misinterpretation (as physically meaningful results) of artifacts due to basis-set inadequacies might well be reduced or avoided by the APW-GTO procedure rather than the standard LCGTO procedure. In any event the 12*s*,8*p*,3*d* set had no comparable deficiency. The customary scrutiny of the eigenvalues of the Bloch overlap matrix was also performed at selected high-symmetry points in the first BZ. No difficulties with the 12*s*,8*p*,3*d* basis were uncovered.

The APW-GTO runs consisted of 13 SAPW iterations followed by nine LCGTO iterations. All but the last LCGTO iteration were performed on a Brillouin-zone mesh of 256 points. The last iteration was on 2048 points. Typically, the iterative cycle was repeated until the changes in the leading Fourier coefficients of the Coulomb and exchange potentials were less than 10^{-5} Ry. Equivalent precision in the straightforward use of the LSU code requires 11 to 12 iterations. On an Amdahl 470/V6II running under the IBM MVS operating

TABLE I. Basis set for neon (12*s*,8*p*,3*d*).

s	*p*	*d*
47 870.213 00	129.802 31	5.0
7355.834 90	30.419 334	0.3
1660.176 20	9.621 517	0.15
460.538 77	3.546 452	
146.038 08	1.414 350	
50.413 86	0.578 893	
18.716 542	0.216 045	
7.397 022	0.12	
2.067 677		
0.775 195		
0.291 76		
0.15		

system, the APW-GTO calculations took between 15% and 20% more time than the corresponding direct LCGTO runs. We feel that this modest investment of machine time is justified by the payoff in having both MT and non-MT results.

Since our earlier APW calculation on Ne which came closest to the experimental cohesive energy and static lattice constant was with $\alpha = \frac{2}{3}$, we began this work with that value. We first calculated the Ne energy bands at the static lattice constant ($a = 7.7$ a.u.) determined from the APW calculation.[21] (The experimental lattice constant after removal of zero-point effects is $a = 8.4348$ a.u. KC used[27] $a = 8.4020$ a.u.) The APW-GTO bands which resulted are shown in Fig. 1 for the valence p band and for the conduction bands up to 4.0 Ry above the valence band. Given the differences in α and a, our results do not seem to be significantly different from those of KC,[26] until one gets to the bands at about +2.0 Ry. There our results at the zone center are reversed from the KC results; we find Γ_{15} below Γ_{12}, not above, although split by about the same amount. Some of the bands at Γ are shown in Table II. To check our results, we performed an APW-GTO calculation for neon with $\alpha = 1$. Again, we found the Γ_{15} level below Γ_{12}. Since this implies a rather different band structure from that given by KC, we decided to do additional checking. Specifically, we were interested in determining whether the reversal of Γ_{15} and Γ_{12} levels was a residual MT effect or due to the specific value of the exchange parameter. For this we took $a = 8.4020$ a.u., the value used by KC, and determined the energy bands by a straightforward LCGTO calculation as well with the APW-GTO procedure. Again we found that the ordering of the levels remained unchanged and the two calculations indistinguishable. The SAPW ordering is preserved in both calculations. We reluctantly conclude that the band-structure diagram in Ref. 26 is incorrect for these levels. We hasten to remark that KC did point out indirectly [compare the KC Table I, which is non-self-consistent (non-SC), with their Fig. 1, which is SC] that the ordering of the Γ_{15} and Γ_{12} levels changes as one proceeds from non-self-consistent to self-consistent calculations. We do not observe such a switch and suspect that some kind of labeling error was made in constructing their Fig. 1. It should be noted that the symmetry of a state must be determined *a posteriori* in the LCGTO cal-

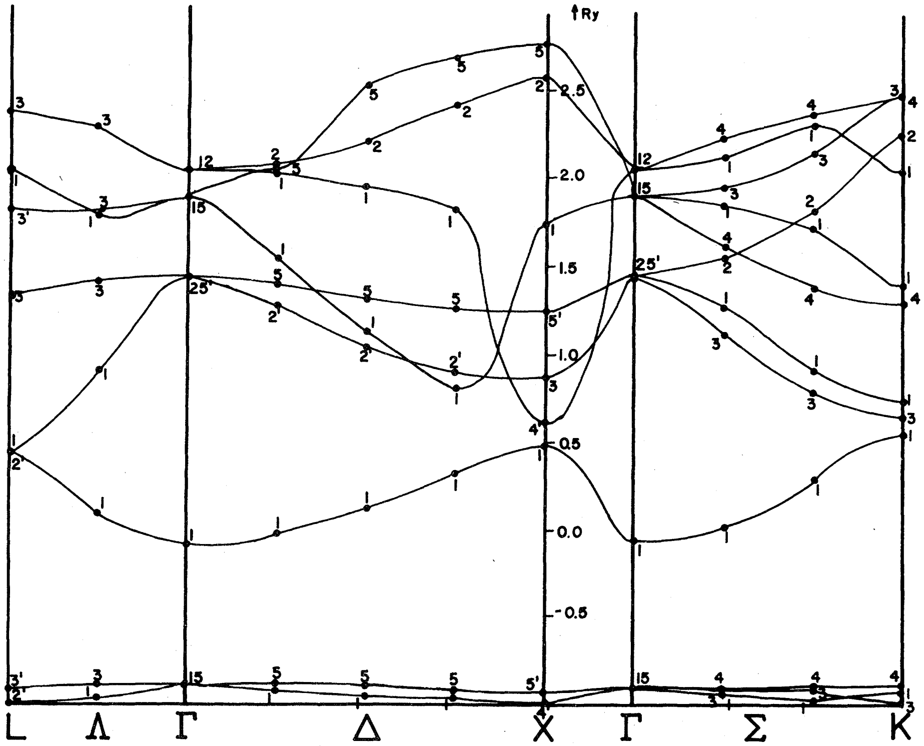

FIG. 1. Self-consistent APW-GTO bands for fcc Ne at $a = 7.7$ a.u. and $\alpha = \frac{2}{3}$. The lowest band shown is the $2p$-like valence band.

TABLE II. Ne energy bands at Γ(Ry) for $a = 7.7$ a.u. and $\alpha = \frac{2}{3}$ and 1 relative to $\Gamma_{15}(2p)$.

Symmetry	SAPW Energy ($\alpha = \frac{2}{3}$)	APW-GTO Energy ($\alpha = \frac{2}{3}$)	SAPW Energy ($\alpha = 1$)	APW-GTO Energy ($\alpha = 1$)
Γ_{15}	0.000 00	0.000 00	0.000 00	0.000 00
Γ_{1}	0.819 51	0.825 31	1.182 23	1.189 88
$\Gamma_{25'}$	2.318 24	2.330 42	2.686 17	2.704 12
Γ_{15}	2.736 03	2.753 43	3.109 69	3.130 78
Γ_{12}	2.869 92	2.895 75	3.209 02	3.245 61

culations, whereas the APW-GTO calculations have the explicit SAPW state symmetry identification available at the start of the GTO iterations. It is difficult to compare our energy levels with other published data[28-31] on Ne bands because of the different computational methods and because of the limited range of energies considered. For example, at Γ, only levels up to $\Gamma_{25'}$ were shown in the band diagrams given in Refs. 29 and 30.

Some measure of the adequacy of our APW-GTO procedure can be obtained from comparison of a few characteristic energy-band quantities. For Ne at $a = 8.542$ a.u., Dagens and Perrot[29] reported a non-SC Hartree-Fock (HF) band gap of 1.87 Ry while Kunz and Mickish[30] reported the SC Hartree-Fock gap as 1.86 Ry. After inclusion of correlation corrections Kunz and Mickish arrived at a calculated band gap of 1.63 Ry. In his review,[32] Rössler quotes the experimental value as 1.58 Ry. Local-exchange models are known to underestimate band gaps in insulators such as these.[33] KC attempted to compensate for that peculiarity by employing $\alpha = 1$ or greater. At $a = 8.4020$ a.u. and $\alpha = 1$ they found a band gap of 1.19 Ry, identical with our APW-GTO result and only 0.01 Ry larger than the SAPW value. Our specific values are in Table III.

We find the same valence bandwidth (0.0302 Ry) from APW-GTO as do KC at $\alpha = 1$ and $a = 8.402$ a.u., a reassuring indication that our procedure and theirs both converged to the same result. The SAPW valence bandwidth at this a and α is 0.0303 Ry.

In the course of these calculations we discovered a characteristic of the LCGTO methodology and practice as implemented in the LSU code which makes it vulnerable to being hung in a self-consistent minimum which does not correspond to the true SC solution of (2.1). By accident, we obtained on one occasion a seemingly proper but actually rather poor set of starting Fourier coefficients for the LCGTO part of the APW-GTO procedure. We were surprised to encounter, at the first iteration, a set of bands which had the $2p$ states somewhat too close to the $2s$ states (as compared with the SAPW results) and the $1s$ states about 25 Ry above their SAPW values. At least briefly we were even more surprised to discover that this glaring dif-

TABLE III. Energies of the bands (in Ry) at Γ of Ne at $a = 8.4020$ and $\alpha = 1$ for LCGTO, APW-GTO, and SAPW.

Symmetry	LCGTO	APW-GTO	SAPW
Γ_{15}	0.000 00	0.000 00	0.000 00
Γ_{1}	1.190 05	1.191 66	1.182 00
$\Gamma_{25'}$	2.520 59	2.525 00	2.510 29
Γ_{15}	2.863 30	2.864 33	2.825 60
Γ_{12}	2.975 77	2.978 81	2.950 74

ficulty would not be remedied by iteration and that these unrealistic states would reach apparent self-consistency in the LCGTO iterative cycle. Such is not the case in our experience with the SAPW code nor with molecular Gaussian orbital codes.

We suspect two sources for the difficulty. The more significant is probably the practice[20] of fixing all but the lowest (in $\vec{K}$) 40 – 60 Fourier coefficients at their zeroth-iteration value. While there is no requirement in principle that this limitation be imposed, there are obvious computational economies if the starting potential is sufficiently realistic. The other source of difficulty with a set of starting Fourier coefficients which is unrealistic lies in the procedure used in the LSU code [note especially the discussion associated with Eq. (20) of Ref. 23] to treat the $\rho^{1/3}$ term in (2.2). As discussed in Ref. 23, $\rho^{1/3}$ at any iteration is approximated as

$$\rho^{1/3}(\vec{r}) = [\rho_0(\vec{r}) + \delta\rho(\vec{r})]^{1/3}$$

$$\approx \rho_0^{1/3}(\vec{r}) + \tfrac{1}{3}\rho_0(\vec{r})^{-2/3}\delta\rho(\vec{r}) , \qquad (3.1)$$

with $\rho_0(\vec{r})$ the zeroth-iteration charge density. Our experience seems to indicate that even fairly subtle deficiencies in ρ_0 [by which we mean deficiencies that are not obvious to an experienced user who inspects a tabulation of $\rho_0(\vec{r})$] will vitiate the linearization (3.1). We suggest that the APW-GTO procedure has at least a modest advantage in avoiding this problem since the potentials and charge density used to start the LCGTO part of the process are rather realistic crystalline quantities.

IV. COMPTON PROFILE

The Compton profile is a measure of the electron momentum distribution. Let $\vec{p}$ denote the initial momentum of an electron in the system, $\vec{\kappa}$ denote the change in momentum after a Compton scattering event has occured, and $\hbar\omega$ denote the energy transferred to the electron. In the impulse approximation, the cross section for scattering into a fixed direction is proportional to [34]

$$J_{\hat{\kappa}}(q) = \frac{\Omega}{(2\pi)^3} \int d\vec{p}\,\rho(\vec{p})\delta(q - \vec{p}\cdot\vec{\kappa}) , \qquad (4.1)$$

in which $\rho(\vec{p})$ is the momentum distribution function, $\hat{\kappa} = \vec{\kappa}/|\kappa|$, and

$$q = m\omega/|\vec{\kappa}| - \tfrac{1}{2}|\vec{\kappa}| . \qquad (4.2)$$

A straightforward procedure exists for evaluation of $J_{\hat{\kappa}}(q)$ using wave functions expressed as combinations of Gaussian orbitals. The details have been discussed previously.[35] A point to remember is the convergence of the reciprocal-lattice sum which appears in these calculations. A check on this convergence can be obtained from the normalization condition of $J_{\hat{\kappa}}$ (q):

$$\int_0^\infty J_{\text{sph}}(q)dq = \frac{n_e}{2} , \qquad (4.3)$$

in which n_e is the number of band electrons per unit cell and J_{sph} is the isotropic Compton profile. In our calculation, the sums over K_s were carried out over 3647 reciprocal-lattice vectors. No contribution was included from the 1*s* wave functions. We note that the impulse approximation is probably not valid for 1*s* electrons anyway. It is also necessary that the electron distribution be sampled at a sufficiently large number of points in the Brillouin zone to give an adequate representation of the momentum distribution function. In the calculations presented here, 2048 points in the full Brillouin zone were employed. We do not expect any discernible change in the values quoted here if more points are used in the zone.

The computed Compton profiles for $a = 7.7$ and $\alpha = \frac{2}{3}$ are given in Table IV for the [100], [110], and [111] directions. The spherically averaged profile is computed from[36,37]

$$J_{\text{sph}}(q) = \tfrac{1}{35}[10J_{100}(q) + 16J_{110}(q) + 9J_{111}(q)] . \qquad (4.4)$$

J_{sph} values for both the APW-GTO calculation and the previous SAPW calculation from this project [22] are given as well in Table IV. For comparison, they are also plotted in Fig. 2. Observe that the 1*s* core contributions to the SAPW profile have been subtracted from the results for the total profile reported in Ref. 22. Except for high values of q, it is noted that $J(q)$ from the straightforward SAPW is slightly higher than the $J(q)$ from the APW-GTO. We also note, as pointed out in Ref. 22, that the calculation of Compton profiles from an SAPW basis is prohibitively expensive, particularly in view of the relatively coarse $\vec{k}$-space mesh. On the other hand, once the APW-GTO self-consistent calculations have been completed, it takes around 12 min

TABLE IV. Calculated Compton profile for neon ($a = 7.7$, $\alpha = \frac{2}{3}$).

q	J_{100}	J_{110}	J_{111}	J_{sph}	J_{APW}
0.0	2.6155	2.6059	2.6143	2.6108	2.6481
0.1	2.6076	2.5978	2.6057	2.6026	2.6481
0.2	2.5828	2.5747	2.5796	2.5783	2.6481
0.3	2.5382	2.5320	2.5342	2.5343	2.5588
0.4	2.4717	2.4665	2.4675	2.4682	2.5290
0.5	2.3825	2.3788	2.3793	2.3800	2.3727
0.6	2.2718	2.2698	2.2707	2.2706	2.3443
0.7	2.1426	2.1445	2.1437	2.1438	2.1811
0.8	1.9993	2.0086	2.0022	2.0043	2.0429
0.9	1.8471	1.8641	1.8517	1.8561	1.8825
1.0	1.6927	1.7135	1.6977	1.7035	1.7397
1.2	1.3967	1.4067	1.3992	1.4019	1.4274
1.4	1.1375	1.1256	1.1350	1.1314	1.1472
1.6	0.9182	0.8994	0.9144	0.9086	0.9274
1.8	0.7363	0.7278	0.7356	0.7322	0.7405
2.0	0.5907	0.5961	0.5917	0.5934	0.6032
2.2	0.4765	0.4871	0.4766	0.4814	0.4817
2.4	0.3858	0.3911	0.3850	0.3880	0.3839
2.6	0.3126	0.3103	0.3122	0.3114	0.3122
2.8	0.2543	0.2490	0.2548	0.2520	0.2544
3.0	0.2091	0.2053	0.2092	0.2074	0.2073
3.2	0.1734	0.1735	0.1729	0.1733	0.1700
3.4	0.1441	0.1474	0.1439	0.1456	0.1420
3.6	0.1201	0.1229	0.1204	0.1215	0.1182
3.8	0.1012	0.1010	0.1014	0.1012	0.0989
4.0	0.0859	0.0837	0.0857	0.0848	0.0822

on an Amdahl 470/V6 to calculate $J(q)$ for $0 \leq q \leq 4$ a.u. in steps of 0.01 along all three symmetry directions. This is a significant saving in computational effort and expense. Because of the increased precision provided by the finer $\vec{k}$ mesh, our results from the APW-GTO calculation are probably much more reliable than the SAPW results. However, because of the lack of any experimental data, no definite conclusion can be reached. Euwema *et al.*[31] found from HF calculations that the Compton profile for Ne is isotropic, consistent with the usual picture of a weakly bound solid of essentially spherical atoms. Their results do indicate, however, a slight variation in $J(q)$ along the different directions. We also found a weak anisotropy in $J(q)$. Directional differences in $J(q)$ are plotted in Figs. 3–5, and a comparison of our values with those of Euwema *et al.*[31] is shown in Table V. To attempt a valid comparison, we have subtracted the core part ($1s^2$ atomic HF Compton profile[38]) from the results in Ref. 31.

V. CONCLUSIONS

We have demonstrated the utility of the APW-GTO hybrid method to determine energy bands. The method is unusual in that we can assess non-muffin-tin effects on band structure as well as cross-check such things as basis-set effects. Compton-profile calculations are facilitated greatly by this method, which turns out to be superior to APW calculations, in so far as computational investment versus reward is concerned. Our results for Ne compared well with those of other workers.

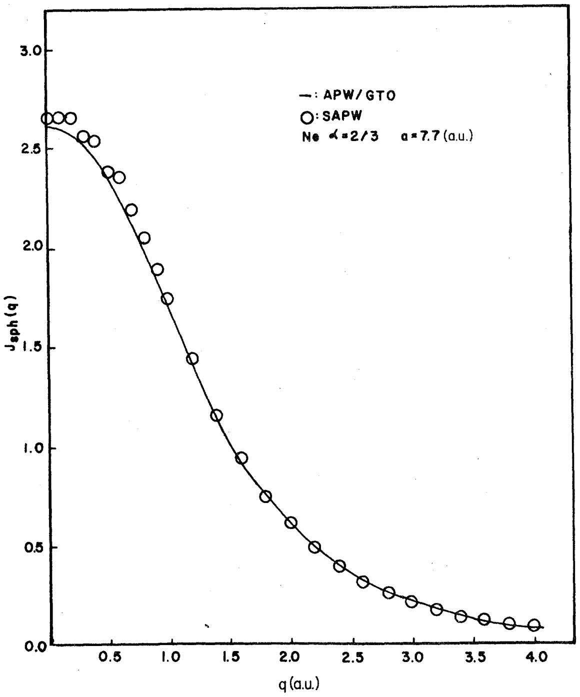

FIG. 2. Spherically averaged Compton profiles for Ne, $a = 7.7$ a.u. and $\alpha = \frac{2}{3}$. Solid curve: this work; open circles: SAPW (Ref. 22).

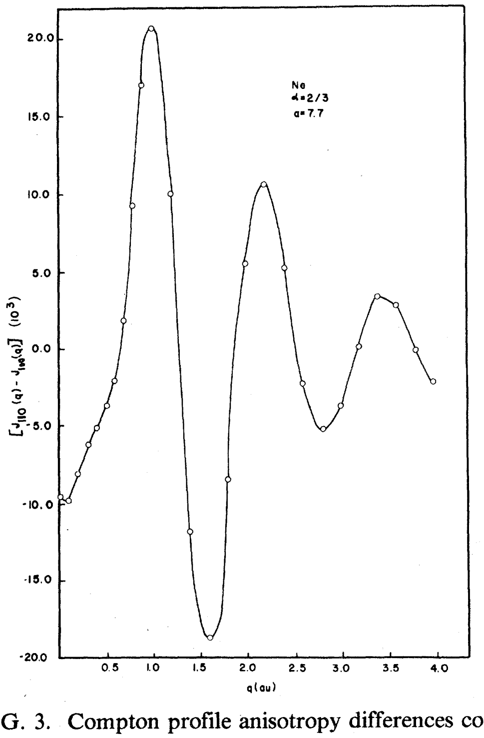

FIG. 3. Compton profile anisotropy differences comparing the [110] and [100] directions.

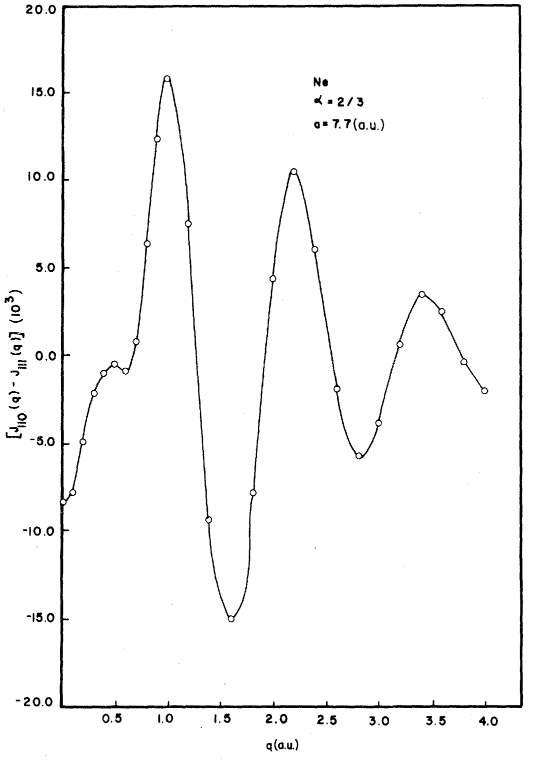

FIG 4. As in Fig. 3 except [110] versus [111].

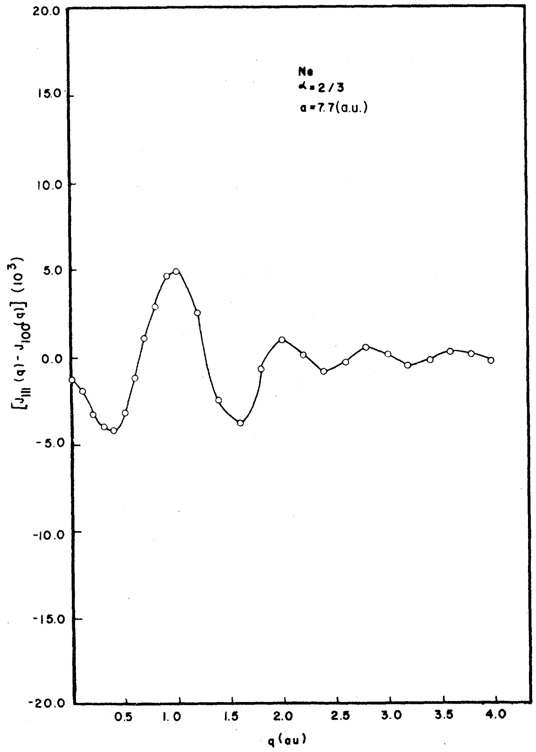

FIG. 5. As in Fig. 3 except [111] versus [100].

TABLE V. Comparison of Compton profiles from APW-GTO and HF calculations. HF results from Ref. 31 with $1s^2$ contribution (Ref. 38) subtracted.

q	APW-GTO J_{100}	HF J_{100}	APW-GTO J_{110}	HF J_{110}	APW-GTO J_{111}	HF J_{111}
0.0	2.6155	2.5422	2.6059	2.5422	2.6143	2.5462
0.1	2.6076	2.5362	2.5978	2.5372	2.6057	2.5402
0.2	2.5828	2.5154	2.5747	2.5174	2.5796	2.5194
0.3	2.5382	2.4746	2.5320	2.4766	2.5342	2.4766
0.4	2.4717	2.4142	2.4665	2.4142	2.4675	2.4092
0.5	2.3825	2.3346	2.3788	2.3316	2.3793	2.3286
0.6	2.2718	2.2354	2.2698	2.2324	2.2707	2.2374
0.7	2.1426	2.1192	2.1445	2.1192	2.1437	2.1302
0.8	1.9993	1.9912	2.0086	1.9962	2.0022	2.0002
0.9	1.8471	1.8552	1.8641	1.8652	1.8517	1.8572
1.0	1.6927	1.7154	1.7135	1.7264	1.6977	1.7104
1.2	1.3967	1.4360	1.4067	1.4350	1.3992	1.4320
1.4	1.1375	1.1800	1.1256	1.1700	1.1350	1.1800
1.6	0.9182	0.9604	0.8994	0.9544	0.9144	0.9584
1.8	0.7363	0.7732	0.7278	0.7752	0.7356	0.7722
2.0	0.5907	0.6192	0.5961	0.6222	0.5917	0.6182

ACKNOWLEDGMENTS

We are grateful to G. P. Alldredge, J. Callaway, D. G. Laurent, and J. P. Worth for several helpful conversations and insights. Computer support from the North East Regional Data Center of the State University System of Florida as well as grant support from the National Science Foundation is also acknowledged with thanks.

---

[1] J. C. Slater, Phys. Rev. 51, 846 (1937). The review most akin to this work is L. F. Mattheiss, J. H. Wood, and A. C. Switendick, in *Methods of Computational Physics,* edited by B. Alder, S. Fernbach, and M. Rotenberg (Academic, New York, 1968), p. 63. See also T. L. Loucks, *Augmented Plane Wave Method* (Benjamin, New York, 1967).

[2] B. Segall and F. S. Ham, in *Methods of Computational Physics,* edited by B. Alder, S. Fernbach, and M. Rotenberg (Academic, New York, 1968), p. 251, and references therein.

[3] H. Schlosser and P. M. Marcus, Phys. Rev. 131, 2529 (1963).

[4] P. D. DeCicco, Phys. Rev. 153, 931 (1967).

[5] W. E. Rudge, Phys. Rev. 181, 1024 (1969).

[6] D. D. Koelling, Phys. Rev. 188, 1049 (1969).

[7] L. Kleinman and R. Shurtleff, Phys. Rev. 188, 1111 (1969).

[8] J. W. D. Connolly, Semi-Annual Progress Report No. 72, p. 26 (Solid State and Molecular Theory Group, MIT, Cambridge Massachusetts, 1970); No. 73, p. 27.

[9] D. D. Koelling, A. J. Freeman, and F. M. Mueller, Phys. Rev. B 1, 1318 (1970).

[10] D. D. Koelling, Phys. Rev. B 2, 290 (1970).

[11] E. O. Kane, Phys. Rev. B 1, 1917 (1971).

[12] N. Elyashar and D. D. Koelling, Phys. Rev. B 13, 5362 (1976); 15, 3620 (1977).

[13] R. Evans and J. Keller, J. Phys. C 4, 3155 (1971).

[14] A. B. Kunz, Phys. Lett. 27A, 401 (1968).

[15] D. E. Ellis and G. S. Painter, Phys. Rev. B 2, 2887 (1970).

[16] A. Zunger and A. J. Freeman, Phys. Rev. B 15, 4716 (1977).

[17] B. I. Dunlap, J. W. D. Connolly, and J. R. Sabin, J. Chem. Phys. 71, 3316 (1979); J. W. Mintmire, Int. J. Quantum Chem. Symp. 13, 163 (1979).

[18] MOLACH program package: hybrid of MOLECULE by J. Almlöf (Uppsale University, Sweden) and ALCHEMY by P. S. Bagus and B. Liu (IBM Research, San Jose, California) with interfacing by P. S. Bagus (IBM) and by U. Walgren (Uppsala).

[19] J. W. Mintmire and J. R. Sabin, Int. J. Quantum Chem. Symp. 14 (in press).

[20] C. S. Wang and J. Callaway, Compt. Phys. Commun.

14, 327 (1978).

[21] J. R. Sabin, J. P. Worth, and S. B. Trickey, Phys. Rev. B 11, 3658 (1975).

[22] J. P. Worth, C. L. Merry, and S. B. Trickey, J. Phys. Chem. Solids. 41, 623 (1980).

[23] J. W. D. Connolly, in *Modern Theoretical Chemistry,* edited by G. Segal (Plenum, New York, 1976) Vol. 7, pp. 105—132, and references therein.

[24] F. Herman and S. Skillman, *Atomic Structure Calculations,* (Prentice Hall, Englewood Cliffs, New Jersey, 1963), Chap. 4.

[25] C. S. Wang and J. Callaway, Comput. Phys. Commun. 14, 330 (1978); 14, 332 (1978).

[26] M. A. Khan and J. Callaway, Phys. Lett. 76A, 441 (1980).

[27] J. Callaway and D. Laurent (private communication).

[28] U. Rössler, Phys. Status Solidi 42, 345 (1970).

[29] L. Dagens and F. Perrot, Phys. Rev. B 5, 641 (1972).

[30] A. B. Kunz and D. J. Mickish, Phys. Rev. B 8, 779 (1973).

[31] R. N. Euwema, G. G. Wepfer, G. T. Surratt, and D. L. Wilhite, Phys. Rev. B 9, 5249 (1974).

[32] U. Rössler, in *Rare Gas Solids,* edited by M. L. Klein and J. D. Venables (Academic, New York, 1975), p. 505; see Table V, p. 545.

[33] S. B. Trickey and J. P. Worth, Int. J. Quantum Chem., Symp. 11, 529 (1977); S. B. Trickey, A. K. Ray and J. P. Worth, Phys. Status Solidi (in press).

[34] P. M. Platzman and N. Tzoar, Phys. Rev. 139, A410 (1965).

[35] J. Rath, C. S. Wang, R. A. Tawil, and J. Callaway, Phys. Rev. B 8, 5139 (1973).

[36] W. V. Houston, Rev. Mod. Phys. 20, 161 (1948).

[37] D. D. Betts, A. B. Bhatia, and M. Wyman, Phys. Rev. 104, 37 (1956).

[38] R. J. Weiss, A. Harvey, and W. C. Phillips, Philos. Mag. 17, 241 (1968).